Detection and Estimation of Multiple Disparities by Multi-evidential Correlation

by

Esfandiar Bandari
& James J. Little

Technical Report 93-38
September 1993

Department of Computer Science
University of British Columbia
Rm 201 - 2366 Main Mall
Vancouver, B.C.
CANADA V6T 1Z4

Telephone: (604) 822-3061
Fax: (604) 822-5485

Detection and Estimation of Multiple Disparities by Multi-evidential Correlation

Esfandiar Bandari and James J. Little

Technical Report 93-38
September 1993

Laboratory for Computational Vision
Department of Computer Science
University of British Columbia
Vancouver, British Columbia, CANADA V6T 1W5
email: bandari@cs.ubc.ca

Abstract

This paper addresses *detection* and *estimation* of multiple disparities in motion and stereo using multi-evidential correlation. No *a priori* knowledge of the presence or the absence of or even the number such disparities is assumed. The procedure utilizes two matching kernels, one based on phase correlation and the other based on a variation of cepstral filtering that provide direct estimates of multiple motion or stereo disparities.

Multi-evidential correlation and the kernels utilized are described and results are presented for motion transparency, occluded boundary and multi-frame analysis of reflected images.

Both kernels were found useful, but phase correlation showed unstable behavior and very broad peaks in the presence of curved surfaces making recognition of multiple disparities difficult. Cepstrum, on the other hand, had very high signal to noise ratio, and provided stable performance thorough all iterations.

Submitted to ECCV'94

1 Introduction

As pointed out pictorially by Bergen, Burt, Higorani and Peleg[BBHP90] different phenomena may result in multiple disparities in a single image neighborhood. Some of these include multiple disparities due to reflection or specularities, relative motion of objects and transparent surfaces in front of them, such as clouds or glass, and multiple motion or stereo disparities at occluded boundaries. Peleg and Irani[IP92] showed an application of multiple motion estimation to track objects through image frames and improve their appearance and resolution over time.

One of the first attempts to find multiple disparities in single image regions was by Fenema and Thompson[FW79] who used a histogram of the correlation results to localize occluded regions within two frames. Since then many researchers have provided more robust and interesting approaches based on a variety of disparity estimation techniques.

Peleg and Rom[PR90], for instance, used an iterative approach for motion segmentation based on constraint equations of brightness change for images where depth of the scene was already known or remained constant. Campani and Verri[CV92] also used the differential approach for optical flow estimation to calculate multiple motion disparities in image sequences.

Darrel and Pentland[DP91] used robust statistics and temporal integration to find distinct "layers" of motion. Jepson and Black[JB93] also used robust statistics and the optical flow gradient constraint equation to find multiple disparities.

Little and Gillet[LG90] used a normalized correlation approach, but introduces two mechanisms to independently determine the occluding boundaries in stereo images.

Burt, Higorani and Kolczynski[BHK], use a Laplacian pyramid and the iterative selective stabilization routine to lock into and cancel a dominant velocity when this velocity is detectable within a frequency band provided by the Laplacian, band-pass, pyramid structure. Bergen, Burt, Higorani and Peleg[BBHP90] also used an iterative approach to determine two constant velocities present in three frames.

Finally, Jones and Malick[JM92] proposed an elegant approach based on the distance measure of vectorized response measures to orthogonal linear filters to determine occluded regions on stereo scenes. Chen, Shirai and Asada[CSA93] also used linear spatial filtering as well as the motion constraint equation to find occluded regions.

In this paper we use multi-evidential correlation to detect the presence of multiple disparities without any *a priori* knowledge of their existence, and to estimate differing disparities due to reflection, transparency and occlusion. The number of disparities present is not limited to two and, as we will see, the matching kernels used, namely phase correlation and cepstrum filtering, provide direct estimates of multiple motion or stereo disparities. Furthermore, in the case of constant velocities, we show how multi-frame analysis can improve the detection and the estimation process by allowing constant disparities among frames to reinforce one another.

In the next section we provide a brief review of multi-evidential correlation and the mathematical properties of the different filters used. We also present examples based on random dot stereograms to provide a quantitative comparison between cepstrum and phase correlation. In section 3 we present results of multiple disparity estimation due to transparent motion and discuss different algorithms to segment a stereo image based on occluded boundary. Finally we discuss the use of a multi-frame analysis technique, called multiCeps, to find constant multiple disparities due to reflection in a sequence of three images.

2 Multi-evidential Correlation, Cepstrum and Phase Correlation

Bandari and Little[BL92, BL] introduced multi-evidential correlation in conjunction with visual echo analysis, and cepstrum filtering.

There are a few filters such as cepstrum[BHT62], phase correlation[KH75] and those based on Hadamard transform[LC88] that provide direct measurement of disparity between two image windows. In the case of cepstrum and phase correlation these measurements are found by locating the Kroenecker delta peak in the resulting filter. The magnitude of these peaks diminish in strength and can be overcome by noise, as the disparity between the two windows increase – i.e., the area of the matching parts between two windows decrease. Multi-evidential correlation [BL92, BL] is an iterative technique which substitutes such filters for sum of absolute or squared differences in a correlation like routine, and therefore provides multiple measurements of motion or stereo disparities in an image neighborhood.

To be more precise, a window from one image centered at (x_1, y_1) is compared against another window from the second frame located at $(x_2, y_2) = (x_1 + \delta_x, y_1 + \delta_y)$ where $\delta_{xmin} \leq \delta_x \leq \delta_{xmax}$ and $\delta_{ymin} \leq \delta_y \leq \delta_{ymax}$ are small offsets that sweep a small discrete range. As a result the window from the first image is compared against a series of windows from a neighborhood in the second image using cepstrum or phase correlation. Most importantly, each time a comparison takes place a new measurement of disparity is collected. Inconsistent measures, or outliers, can then be discarded and the remaining measurements can then be combined and confidence measures calculated. We have found that a more efficient approach is to find a few evidences that point to a particularly disparity, then extract and compare the two overlapping windows based on this estimate, and make sure that their disparity corresponds as closely as possible to (0, 0) motion. For a more detailed discussion the reader is referred to [BL93b].

An important property of cepstrum and phase correlation is that they both produce multiple peaks in the presence of multiple motions within a window. Figure 1 shows a manufactured image to display the effects of multiple motion on phase correlation and cepstrum. The box in the image was move by 3 pixels vertically and 6 pixels horizontally, while the main image was moved 10 pixels vertically and 5 pixels horizontally. These motions created the corresponding peaks in the cepstrum result, a relevant portion of which is shown topographically, with the two peaks estimating the correct disparity.

This property, in conjunction with multi-evidential correlation, provides a unique approach to detection and recognition of multiple disparities when they are present. To elaborate, when two or more disparities appear in an image, they generate two or more peaks in cepstrum and phase correlation. As multi-evidential correlation sweeps a window from one frame over a region in the other, only the peaks corresponding to legitimate disparities persist, each of them indicating a consistent disparity measure. The relative magnitude of these peaks will, of course, increase and decrease as the relative overlapping areas of the matching image parts decrease or increase. But the peaks themselves persist over all or some part of the iteration. In this manner we can first *detect* the presence of multiple disparities and then estimate their proper values.

In the following subsections we describe phase correlation and a variation of power cepstrum for estimation of motion and binocular disparity. We defer the mathematical treatment of their behavior in the presence of multiple motion and instead provide

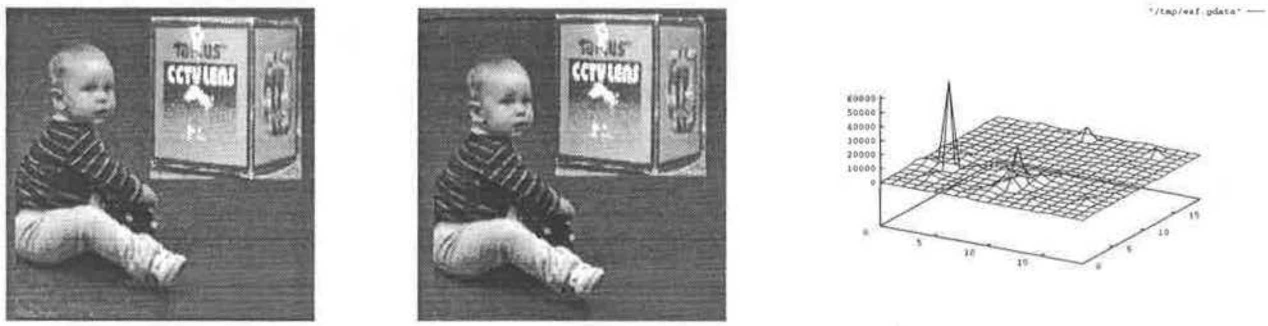

(a) (b) (c)

Figure 1: (a) & (b) the manufactured images. (c) the result of analyzing the images with cepstrum or phase correlation.

examples based on random dot stereograms.

2.1 Phase Correlation and Multi-evidential Correlation

Phase Correlation was first introduced by Kuglin and Hines[KH75] as an image alignment methodology. Given two image windows $s_1(x, y)$ and $s_2(x, y)$ their phase correlation is defined as:

$$\mathcal{F}^{-1}\{\frac{\mathcal{S}_1(\omega_x, \omega_y) \cdot \mathcal{S}_2^*(\omega_x, \omega_y)}{|\mathcal{S}_1(\omega_x, \omega_y) \cdot \mathcal{S}_2^*(\omega_x, \omega_y)|}\} \tag{1}$$

where $\mathcal{S}_1$ and $\mathcal{S}_2^*$ are the Fourier transform and the conjugate Fourier transform of the s_1 and s_2 respectively, and $\mathcal{F}^{-1}$ is the inverse Fourier transform of the result. The denominator of this equation is the amplitude of the numerator; thus given two windows that are shifted with respect to each other by (d_x, d_y), it is easy to show that the result of this normalized correlation in the Fourier domain is simply $e^{i(d_x\omega_x + d_y\omega_y)}$. The inverse Fourier transform of this exponential will then result in a sharp Kroenecker delta peak at (d_x, d_y).

It can also be shown mathematically that if multiple disparities are present in the two windows, phase correlation results in multiple peaks corresponding to the individual disparities plus a small residual noise. To show this effect, and how multiple

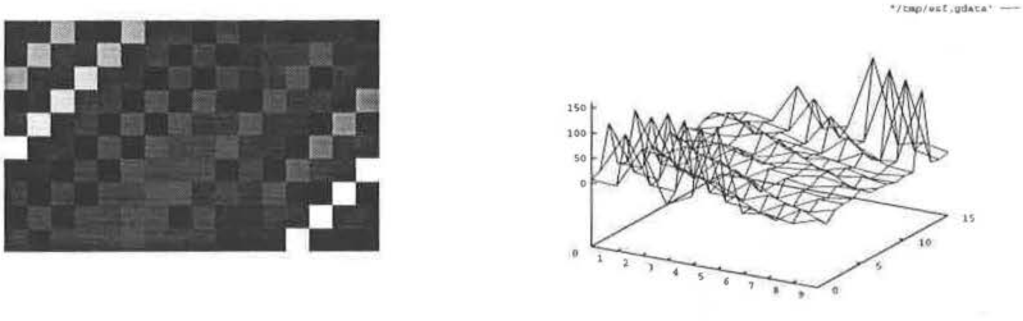

(a) (b)

Figure 2: (a). Each row of the figure represents the result of one iteration of the multi-evidential correlation with phase correlation as its matching kernel. The location of the peaks are indicative of the disparity, with negative disparities located from the left column. (b) Topographic image of figure (a) displaying the magnitude of the phase correlation peaks

peaks persist over individual iterations of multi-evidential correlation, we generated a random dot stereogram with two disparity levels of 2 and 5. We then chose an area near the occluded boundary, and using phase correlation as the matching kernel we conducted multi-evidential correlation. For window size, we chose 16 by 16 pixels size patches[1] and for the correlation span (i.e., the area which we sweep over during our comparison) we selected 0 to 10 columns horizontally and zero columns vertically. Since epipolar constraint was preserved, and our motion (or span) was only horizontal, the peaks in each phase correlation outcome appear only on the first row of the inverse Fourier transform, thus reflecting 0 vertical disparity. We then kept the first row of each phase correlation result in our multi-evidential correlation and concatenated them together vertically. Figure 2 shows the result with each row representing the outcome of one phase correlation match.

As can be seen, each row contains two peaks corresponding to the two disparities. As we move to the right these disparities get smaller by one pixel, as expected, and

[1]Eight pixels by eight pixels windows or even smaller window sizes would also be adequate, but we chose a larger size for display purposes.

reach their respective maximum magnitudes at 0 disparities (i.e., when they reach the left hand column). If we continue moving to the right the peaks reappear in the right hand column, indicating a negative disparity, and their magnitude again starts to decrease with each iteration.

What is important to note is the consistent presence of the two peaks and how their relative location moves as we iterate over an area. If such consistency persists during multi-evidential correlation over an image neighborhood then it is easy to infer that multiple disparities due to occlusion, reflection, or transparency has occurred.

Even though the example presented here corresponds to binocular disparity (primarily for proper visualization), the same approach can be extended to the detection and estimation of two or more motion disparities.

2.2 cepsCorr: Cepstrum and Multi-evidential Correlation

Power cepstrum was first introduced by Bogert, Healy and Tuckey[BHT62] to determine the delay arrival period of echoes in time. Described briefly, power cepstrum is the power spectrum of the log of the power spectrum of a signal.

$$|\mathcal{F}\{\ \log(\ \mathcal{F}\{s(x,y)\}\ )\ \}| \tag{2}$$

Since its introduction, different variations to cepstrum such as complex cepstrum, phase cepstrum [SC75] and differential cepstrum[RR87] have been developed for detection, retrieval, and removal of echoes, as well as for homomorphic filtering, deconvolution and image restoration.[2] We have examined different cepstrum techniques and found that a variation of power cepstrum, called cepsCos, which replaces the second power spectrum with cosine transform to be the best approach for determination of signal disparities[BL93a].

We next used cepstrum as the correlation kernel in our multi-evidential routine – which we often refer to as cepsCorr for brevity – and repeated the experiment described in the previous section. As with the phase correlation the peaks of the cepstrum appear only in the first row of each iteration,, and hence they can be concatenated to one another. Since we use the same windowing routine described in [BL], and since the

[2] For a more detailed discussion of these variations and applicability of cepstrum please refer to [CSK77] and [BL93b].

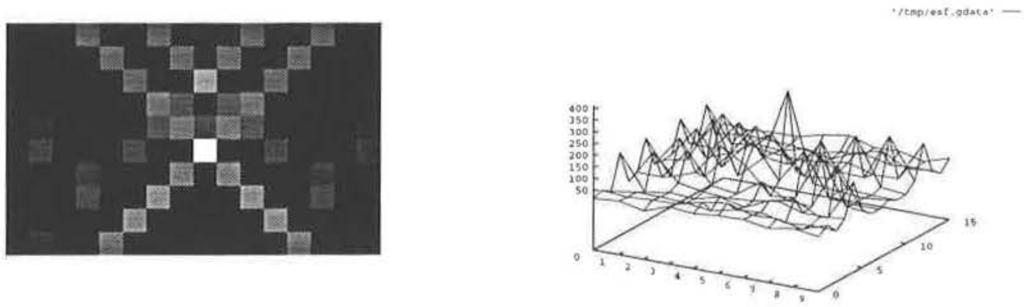

(a) (b)

Figure 3: (a). The collection of binocular disparity signals generated by cepsCorr. Each row of the figure represents the result of one iteration of the multi-evidential correlation with cepstrum as its matching kernel. Each disparity is represented by two peaks which are symmetrically displaced away from the center of column by the disparity. (b) Topographic image of cepsCorr in (a) in order to display the magnitude of the cepstrum peaks.

cepstrums (or cepsCos) of real signals are symmetric and even functions, for binocular disparity the first row of cepstrum will contain two symmetric peaks around the center column for each of the disparities present. Figure 3 shows the cepsCorr results for the experiment described above. Note that, as with phase correlation, as the disparity between two identical parts in the two images reduces, the peak magnitude of their disparity increases, and the peaks move close to the middle column (i.e., zero disparity).

Comparing the two topographic maps in figures 2 and 3 for our matching kernels indicates that the disparity peaks generated by the cepstrum filter are larger in magnitude than those generated by phase correlation by roughly a factor of three to one. Moreover, our experiments indicate that cepstrum results seem to have higher signal to noise ratios than those of phase correlation.

We also encountered instabilities in phase correlation performance which we are investigating further. One of these anomalies, for instance, was the presence of a checkered pattern at certain relative disparities between the two windows. Other researchers[LMK89] have also shown that cepstrum performs better than phase correla-

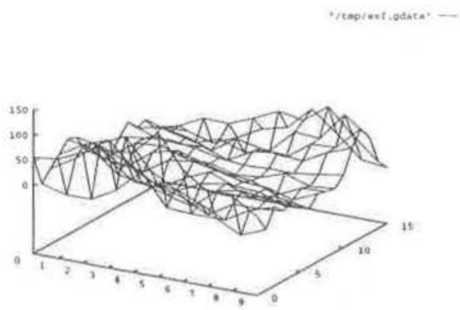

(a)

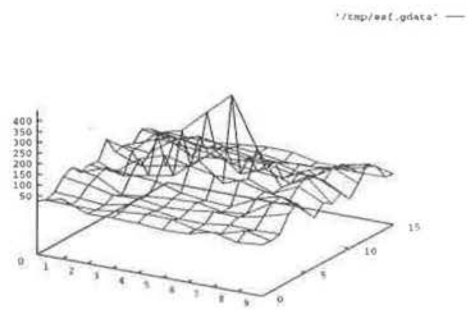

(b)

Figure 4: (a). Topographic representation of multi-evidential correlation results for the pepsi scene with phase correlation as the matching kernel. (b). result of cepsCorr for the same image area in the pepsi scene. Note that cepsCorr generates a strong peak in the center corresponding to one of the disparities while for phase correlation the results are very weak and lack a distinguishing structure.

tion in the presence of noise. Lastly, figures 4 (c) are the results of the same operations as above on the boundary of the real image depicted in figure 7. The estimated peaks in phase correlation, even after taking into account spreading due to the curvature of the Pepsi can was quite inaccurate, while cepstrum's results were much better suited for further analysis.

3 Results

In this section we will apply multi-evidential correlation to the detection of multiple disparities. The three examples that we will tackle are due to motion transparency, detection and localization of occluding boundaries in binocular stereo, and multi-frame analysis of constant dual disparities due to reflection.

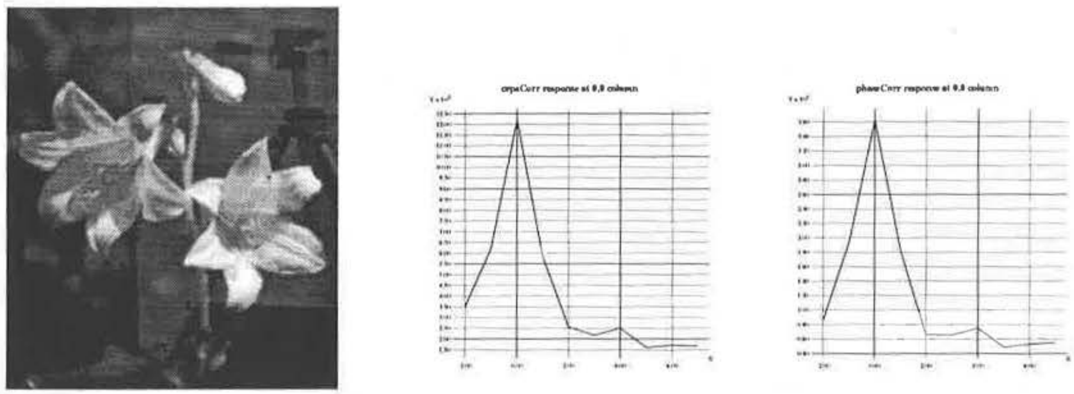

(a) (b) (c)

Figure 5: (a). The first frame of a sequence of motion transparency images. (b). & (c). The magnitude of multi-evidential correlation at (0,0) disparities for cepstrum (b), and phase correlation (c).

3.1 Motion Transparency

Determination of the motions of two objects where one object is transparent and in front of the other is often referred to as the motion transparency solution. One of the applications of this work is matching of satellite images where thin cloud cover or smoke can overshadow the primary matching disparity estimates. Irani and Peleg[IP92] also showed how they used results of motion transparency to track objects behind stained glass and improved the clarity and resolution of the object images over time.

Figure 5 (a) shows an image of a sequence where a tripod is moving behind a window with a picture of flower.

In the first two frames of this sequence, while the flower stays stationary, the tripod moves by 4 pixels horizontally (again there is no vertical motion present). We used phase correlation and cepstrum as the matching kernels for our approach and then checked for maximum peaks at zero disparities – i.e., when the either tripods or the flowers in the two images overlapped. We also chose rather large windows of 128x128 pixels to ensure that both disparities are included in our our analysis. The span of our routine was from -2 to 7 pixels horizontally. The results of the (0,0) peaks are shown in figure 5 (b) and (c). The main two peaks appear at the proper locations and correspond to the offsets where either the flower or the tripod overlap. It is important to note that even though the disparity in this case was only horizontal this is not at all a requirement, and that vertical as well as horizontal disparities can be found quite easily.

3.2 Occluded Boundary

Recognition of occluded boundaries in motion or stereo plays a significant role in segmentation of three dimensional objects. Such segmentation are in turn important for tracking, recognition, or object manipulation in robotics applications.

As we have demonstrated, in the region near an occluded boundary, both phase correlation and cepstrum generate two peaks corresponding to the two disparities present. But while detection and estimation of disparities is easy, localization of the occluded boundary is a more cumbersome task. The primary problem is the duality in detection and localization, as they relate to the window size. Large window sizes are generally better in detection and estimation, but produce greater uncertainty in the location of the edges. Figure 6 shows the uncertainty in locating the occluded boundary of random dot stereograms for two squares.

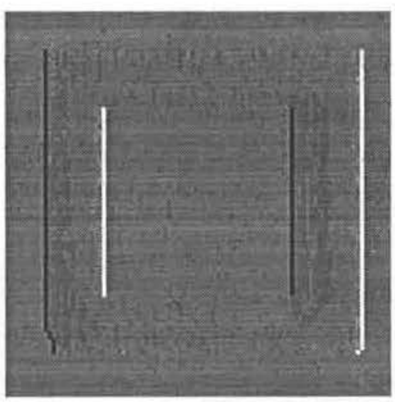

Figure 6: Detection vs. localization of occluded boundary for random dot stereogram. The area between a pair of white and black edges corresponds to the locations where multiple disparities were detected.

This problem is aggravated, and the consistency of multiple peaks in multi-evidential

(a) (b) (c)

Figure 7: (a) & (b) A pair of streo images of a curved object. (c) the occlude boundary of the object using multi-evidential correlation.

correlation is jeopardized, if the window shape does not match the occluded boundary, or if one or both objects in view contain curved or slanted surface structures; this is primarily due to the fact that a curved surface will have multiple disparities within a window which result in a blurring of the disparity peak.

The natural answer to this problem is to use a smaller window size. This approach was examined by Okutomi and Kanade[OK92] who used windows with locally adaptive extents. Our experience with phase and cepstrum indicates however, that even with smaller windows, the window width generates an uncertainty in the location of the occluded area.

It should also be pointed out here that relative sizes of image patches that give rise to mulitple disparities are not the only factors effecting the relative peak magnitudes. Our studies show that other factors such as the relative frequency distribution content of the image windows also play a significant role. Moreover, often the objects creating an occluded boundary are similar in nature, making the detection and localization of the occluded boundaries even more difficult. This is why random dot stereograms are not a good representative problem. An engineering solution that will work with real scenes is to first find edges in the image[3] and then determine if the edge is an occluded

[3] Obviously with an edge finder that has good localization characteristics such as [RHKvdH92].

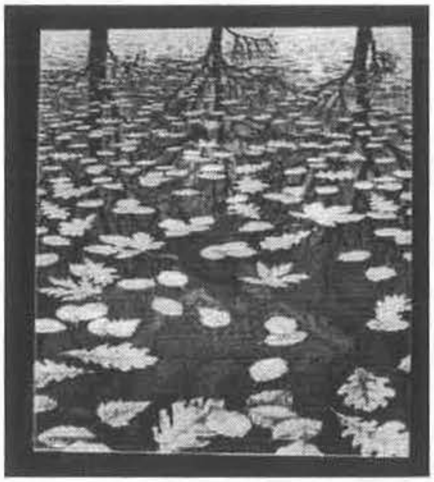

(a)

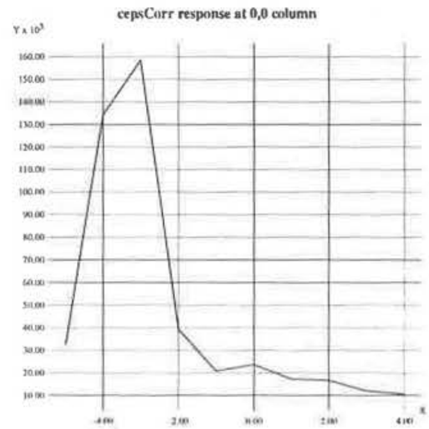

(b)

Figure 8: (a). One of the three images with two constant disparities caused by reflection. (b). The magnitude of the (0,0) peaks caused by the overlap of individual mulitple disparities. Note that the graph shows two maximums due to two disparities.

boundary or a surface feature based on the existence or lack of strong multiple peaks along the edge. The difference between the two disparities, indicates the width of the occluded area.

Instead, we examined different direct methodologies for the detection of occluded boundaries, including voting schemes, and thresholding of relative peak magnitudes. Our final approach to solving the occlusion problem is similar to a technique used by Fua[Fua91] to verify correct disparity calculations. That is, using multi-evidential correlation we selected the largest of the two dominant peaks and centered a stationary window in the second image at that location. We then tried to find the disparity for this window in the first image using multi-evidential correlation. It is easy to show geometrically that (if the information content of the two disparity areas are similar) the verification procedure fails inside an occluded region. In fact, in the occluded regions the secondary peak in the first pass becomes the dominant peak in the second.

Figure 7 shows a pair of stereo images and the occluded boundaries found by the above technique. Where the image lacks features for matching (such the lower part of the pepsi can) this procedure also shows lack of consistency in results. One way to reduce the noise in this result is to verify the existence of multiple peaks for all occluded pixel candidates.

3.3 MultiCeps and Multiple Motion Due to Reflection

In [BBHP90] Bergen, Burt, Higorani and Peleg used an iterative technique to determine two constant motion disparities from three frames. As we can see in figure 8, the magnitudes of the (0,0) disparity peaks in cepsCorr also indicate the presence of at least two motions between frames two and three of the three frame sequence.

In this section we use multi-frame analysis technique called multiCeps[BL] to estimate the constant disparities among the three frames. To do this we concatenate the three frames[4] and conduct cepstral analysis. It is easy to show mathematically that in multiCeps the constant disparities between the first and the second frame and the disparity between the second and third frame reinforce one another. The same results will hold for the disparity between the first and third frame. Figure 9 below shows a small portion of the multiCeps result.

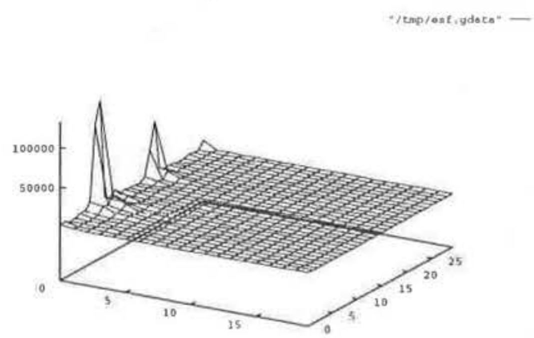

Figure 9: A portion of the cepstrum result for multi-frame analysis.

Close examination of these results shows three peaks corresponding to the three horizontal disparities at -3.4, -0.6 and 6.7 using linear interpolation between the peaks. The first two peaks correspond to the multiple disparity measures (of the Escher print and the reflection) between the first frame and the second frame, reinforcing similar

[4] Actually we used a 341 by 256 sub-image of the three figures.

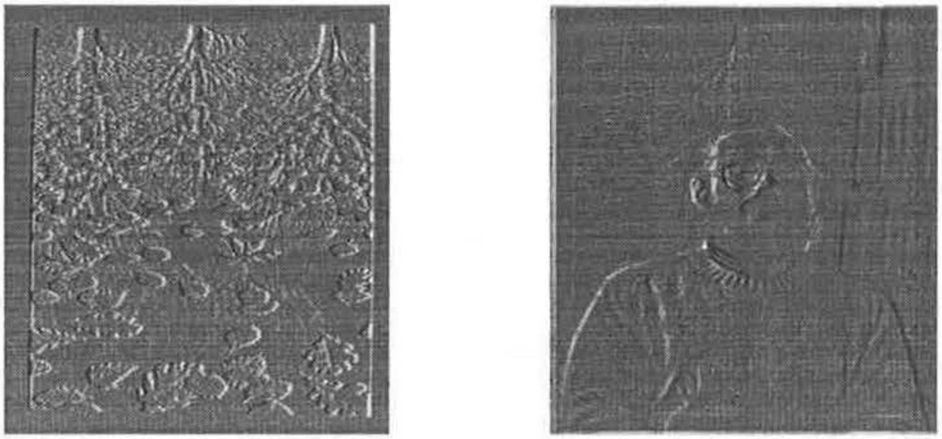

(a) (b)

Figure 10: The difference images between frame 1 and 2 after disparity compensation for the two estimates.

disparities between frames two and three. The last disparity corresponds to one of the two disparities between frame one and frame three. The vertical disparities between these images are also zero. Figures 10 show the outlines of the two images generated by simple subtraction of the first two frames after proper disparity realignment.

The procedure above shows how multi-frame analysis can be utilized in estimation of constant multiple disparity measurements.

4 Conclusion

In this paper we discussed a direct method for detection and estimation of multiple disparities due to occlusion, motion transparency, and reflection using multi-evidential correlation. No *a priori* assumptions about the existence or the number of disparities were made. The two matching kernels used, cepstrum and phase correlation, both generate multiple peaks in the presence of multiple motions. When these peaks persist between different iterations of multi-evidential correlation, and they are consistent in measurement of the disparities, the existence of mulitple disparities is assured.

We also addressed the use of multi-frame analysis and cepstrum to estimate multiple constant disparities over time.

Both cepstrum and phase correlation performed well, but cepstrum had higher signal to noise ratio, and an overall better performance than phase correlation.

A significant fact that should be point out here is that motion transparency and reflection often cause blurring in the image. Both cepstrum and phase correlation are robust to blurring, and in fact cepstrum is often used as a deblurring mechanism.

Acknowledgement: We would like to thank Bob Woodham for his fruitful comments on the draft of this paper. We would also like to thank Shmuel Peleg and Allen Jepson for providing us with interesting test images.

References

[BBHP90] J.R. Bergen, P.J. Burt, R. Higorani, and S. Peleg. Computing two motins from three frames. In *Proceedings of IEEE International Conference on Computer Vision*, pages 27–32, Osaka, Japan, dec 1990. IEEE, Los Alamitos, CA.

[BHK] Peter J. Burt, Rajesh Higorani, and Raymond J. Kolczynski. Mechanism of isolating component patterns in the sequential analysis of multiple motion. In *Proceedings of IEEE Workshop On Visual Motion.*

[BHT62] B.P. Bogert, M.J.R. Healy, and J.W. Tukey. The quefrency analysis of time series for echoes: Cepstrum, psuedo-autocovariance, cross-cepstrum and saphe cracking. *Proc. of Symp. On Time Series Analysis*, 1962.

[BL] Esfandiar Bandari and James J. Little. Visual echo analysis. In *Proceedings of Fourth International Conference in Computer Vision (ICCV).*

[BL92] Esfandiar Bandari and James J. Little. Spatial-queferency approach to optical echo ananlysis. In *Proceedings of Computer Vision and Pattern Recognition (CVPR)*, pages 850–852, Champaign, Illinois, 1992. IEEE, Los Alamitos, CA.

[BL93a] E. Bandari and J.J. Little. Cepstral methods in computational vision. In *Nonlinear Image Processing IV; Proc. SPIE*, San Jose, CA, February 1993. SPIE, Bellingham, WA.

[BL93b] E. Bandari and J.J. Little. Multi-evidential correlation and visual echo analysis. Technical Report TR 93-1, University of British Columbia, 1993.

[CSA93] H. J. Chen, Y. Shirai, and M. Asada. Obtainig optical flow with multi-orientation filters. In *Proceedings of International Conference in Computer Vision and Pattern Recognition*, page 736, New York, New York, 1993. IEEE, IEEE, Los Alamitos, CA.

[CSK77] D.G. Childers, D.P. Skinner, and R.C. Kemerait. The cepstrum: a guide to processing. *Proc. IEEE*, 65(10), October 1977.

[CV92] M. Campani and A. Verri. Motion analysis from first order properties of optical flow. *CVGIP. Image Understanding*, 56(1):90–107, July 1992.

[DP91] T. Darrell and A. PENTLAND. Robust estimation of a multi-layered motion representation. In *Proceedings of the IEEE Workshop on Visual Motion*, pages 173–8. IEEE, Los Alamitos, CA, 1991.

[Fua91] Pascal Fua. A parallel stereo algorithm that produces dense depth maps and pres erves image features. Technical Report 1369, INRIA, January 1991.

[FW79] C.L. Fennema and W.B.Thomson. Velocity determination in scenes containing several moving objects. *Computer Graphics and Image Processing*, 9:301–315, 1979.

[IP92] Michal Irani and Shmuel Peleg. Image sequence enhancement using multiple motions analysis. In *Proceedings of Computer Vision and Pattern Recognition (CVPR)*, pages 216–221, Champaign, Illinois, june 1992. IEEE, Los Alamitos, CA.

[JB93] Allen Jepson and Michael Black. Mixture models for optoical flow computation. Technical Report 93-44, RBCV, November 1993.

[JM92] David Jones and Jitendra Malik. A computational framework for determining stereo correspondence from a set of linear spatial filters. In *Proceedings of Second European Conference on Computer Vision.* Springer-Verlag, 1992.

[KH75] C.D. Kuglin and D.C. Hines. The phase correlation image alignment method. *Proc. IEEE Int. Conf. on Cybernetics and Society*, pages 163–165, 1975.

[LC88] S.H. Lai and S. Chang. Estimation of 2-d translation via hadamard transform. In J.L. Lacoume, A. Chehikian, N. Martin, and J. Malbos, editors, *Signal Processing IV: Theories and Applications. Proc. of EUSIPCO-88. Fourth European Signal Processing Conference*, volume 1, pages 35–37. North-Holland, sept 1988.

[LG90] J. J. Little and W. E. Gillett. Direct evidence of occlusion in stereo and motion. In *European Conference in Computational Vision*, pages 336–340, Antibes, France, April 1990.

[LMK89] D.J. Lee, S. Mitra, and T.F. Krile. Analysis of sequential complex images, using feature extraction and two-dimensioanl cepstrum techniques. *J. Opt. Soc. Am.*, 6(6), 1989.

[OK92] M. Okutomi and T. Kanade. A locally adaptive window for signal matching. *International Journal of Computer Vision*, 7(2):143–162, January 1992.

[PR90] S. Peleg and H. Rom. Motion based segmentation. In *Proceedings of IEEE Tenth International Conference on Pattern Recognition*, pages 109–113, Osaka, Japan, june 1990. IEEE, Los Alamitos, CA.

[RHKvdH92] L. Rosenthler, F. Heitger, O. Kübler, and R. von der Heydt. Detection of general edges and key points. In *Proceedings of Second European Conference on Computer Vision.* Springer-Verlag, may 1992.

[RR87] G.R. Reddy and V.V. Rao. Signal delay and waveform estimation through differential cepstrum averaging. *IEEE Trans. Acoust., Speech, and Signal Processing*, 35(10):1487–89, October 1987.

[SC75] D.P. Skinner and D.G. Childers. The power, complex and phase cepstra. In *Proc. National Conf. on Telecommunication*, December 1975.